

Microscopic Large Scale *psd* Shell Model with M3Y Residual Interaction to Calculate Electron Scattering Form Factors

Khalid S. Jassim* and Rawaa A. Abdul-Nabe

Department of Physics, College of Education for Pure Science, University of Babylon,
 P.O. Box 4, Hilla-Babylon, 00964, Iraq

The longitudinal and the transverse electron scattering form factors for ${}^6\text{Li}$, ${}^9\text{Be}$, ${}^{11}\text{B}$ and ${}^{12}\text{C}$ nuclei have been studied with and without core polarization effects using shell model calculations. The *psdmwk* is used as effective interaction for *psd*-shells. The core-polarization effects are calculated in the first-order perturbation theory including excitations up to $4\hbar\omega$ using the Michigan three-range Yakawa M3Y as a realistic interaction. The wave functions of radial single particle matrix elements have been calculated with harmonic oscillator potential. For all nuclei under studying, Comparison between experimental and theoretical calculations show that the form factors with core-polarization effect calculations give good consistency with experiment data. So we concluded that the large scale model space enhanced the results to become closed to the experimental data.

KEYWORDS: p-Shell Nuclei, Longitudinal Form Factors, Transverse Form Factors, NuShell, Nuclear Structure.

1. INTRODUCTION

The scattering of electrons by nucleus is used to explain the nuclear structure and so supply us the most specific information about the size and charge distribution of nucleus.¹ The electron scattering process can be explained according to the first Born-approximation (FBA) as an exchange of a virtual photon carrying a momentum q between the electron and the nucleus.^{2,3} The first Born-approximation is being valid only if a $Z \ll 1$, where Z is the atomic number and a is the fine structure constant. Depending on this approximation, there are two kinds of electron scattering from the nucleus are clear. The first kind is the transverse form factor which contain the information about the magnetization distributions and nuclear current. In this way the electron interacts with the current distribution and magnetization, where the method is considered as a default photon exchange with angular momentum ± 1 along q direction. The second kind is the longitudinal (Coulomb) scattering. These methods contains all information about the nuclear charge distribution and the electron interacts with the charge distribution of the nucleus, whereas the interaction is regarded as a default photon exchange with zero angular momentum along (q) direction. The transverse form factor according

to the parity selection rules can be sorted into transverse electric and magnetic form factor.⁴ The realistic nucleon–nucleon (NN) realistic (M3Y) interaction is used for core-polarization (CP) effect calculations with microscopic theory.⁵ The single particle matrix elements have been calculated with Harmonic Oscillator (HO) potential.

Recently, Jassim et al.^{5–10} have been completed many studies about nuclear structure of some nuclei in p, sd and fp model space using shell model calculations. These studies give good agreement in energy levels and electron scattering form factors calculations comparing with the experimental data. Majeed et al.¹¹ have been studied the Longitudinal and transverse electron scattering form factors for some positive and negative parity states of stable odd-A nuclei (${}^7\text{Li}$, ${}^{13}\text{C}$ and ${}^{17}\text{O}$) by considering the higher energy configurations outside the p-shells. The ground-state spins and parities of the odd-A phosphorus isotopes ${}^{25-47}\text{P}$ were studied with the relativistic mean-field (RMF) model and relativistic elastic magnetic electron-scattering theory (REMES) by Ref. [12].

The purpose of the present work is to account the longitudinal and the transverse electron scattering form factors with the effect of the CP. The one body density matrix (OBDM) elements calculations have been performed using large scale model space to include the *psd* shells. Two shell model codes, CPM3Y and nushell for windows have been use in our calculations. The large scale two-body (*psdmwk*) effective interaction is used with M3Y as a residual interaction for the CP calculation. The *psdmwk*

*Author to whom correspondence should be addressed.
 Email: Khalid_ik74@yahoo.com
 Received: 27 November 2015
 Accepted: 3 January 2016

effective interaction has the $1p_{3/2}$, $1p_{1/2}$, $1d_{5/2}$, $2s_{1/2}$ and $1d_{3/2}$ shell model wave function which is used for ${}^6\text{Li}$, ${}^9\text{Be}$, ${}^{11}\text{Be}$, ${}^{12}\text{C}$ in this study. The wave function of radial single matrix elements have use Harmonic Oscillator (HO).

2. THEORY

The reduced matrix elements of the electron scattering operator \hat{T}_Λ^η consist of two parts, one is for the Model Space (MS) matrix elements and one for the CP matrix elements.¹³

$$\langle X_f | \|\hat{T}_\Lambda^\eta\| | X_i \rangle = \langle X_f | \|\hat{T}_\Lambda^\eta\| | X_i \rangle_{MS} + \langle X_f | \|\delta\hat{T}_\Lambda^\eta\| | X_i \rangle_{CP} \quad (1)$$

where the state $|X_i\rangle$ and $|X_f\rangle$ are described by the model-space wave functions. Greek symbols are used to denote quantum numbers in coordinate space and isospin, i.e., $X_i \equiv J_i T_i$, $X_f \equiv J_f T_f$ and $\Lambda \equiv J T$.

The MS matrix elements are expressed as the sum of the product of the one-body density matrix elements (OBDM) times the single-particle matrix elements, which is given by:

$$\langle X_f | \|\hat{T}_\Lambda^\eta\| | X_i \rangle_{MS} = \sum_{\alpha, \beta} O_{X_i X_f}^X(\alpha, \beta) \langle \alpha | \|\hat{T}_\Lambda^\eta\| | \beta \rangle_{MS} \quad (2)$$

where α and β denote the final and initial single particle states respectively (isospin is included) for the model space. $O_{X_i X_f}^X$ are the OBDM elements.

Similarly, the CP matrix element can be written as

$$\langle X_f | \|\delta\hat{T}_\Lambda^\eta\| | X_i \rangle_{CP} = \sum_{\alpha, \beta} O_{X_i X_f}^X(\alpha, \beta) \langle \alpha | \|\delta\hat{T}_\Lambda^\eta\| | \beta \rangle_{CP} \quad (3)$$

By using the first order perturbation theory, the single-particle matrix element for the higher-energy configurations outside the core and MS is given by:¹⁴

$$\begin{aligned} \langle \alpha | \|\delta\hat{T}_\Lambda^\eta\| | \beta \rangle &= \langle \alpha | V_{12} \frac{P}{E_i - H^{(0)}} \hat{T}_\Lambda^\eta | \beta \rangle \\ &+ \langle \alpha | \hat{T}_\Lambda^\eta \frac{P}{E_f - H^{(0)}} V_{12} | \beta \rangle \end{aligned} \quad (4)$$

where P is the projection operator onto the space outside the model space and V_{12} are adopted as a residual two-body interaction. E_i and E_f are the energies of the initial and final states, respectively. $H^{(0)}$ is the unperturbed Hamiltonian. Equation (4) is written as¹⁴

$$\begin{aligned} \langle \alpha | \|\delta\hat{T}_\Lambda^\eta\| | \beta \rangle &= \sum_{\alpha_1, \alpha_2, \Gamma} \frac{(-1)^{\beta+\alpha_2+X}}{e_\beta - e_{\alpha_1} - e_{\alpha_2}} (2X+1) \\ &\times \begin{Bmatrix} \alpha & \beta & \Lambda \\ \alpha_2 & \alpha_1 & X \end{Bmatrix} \times \langle \alpha \alpha_1 | V_{12} | \beta \alpha_2 \rangle_X \\ &\times \langle \alpha_2 | \|\hat{T}_\Lambda^\eta\| | \alpha_1 \rangle \\ &\times \sqrt{(1 + \delta_{\alpha_1 \alpha}) (1 + \delta_{\alpha_2 \beta})} + A \end{aligned} \quad (5)$$

where A represents additional terms with α_1 and α_2 exchanged with an overall minus sign. The indices α_1 and

α_2 run over particle and hole states, respectively, and e is the single-particle energy. The CP parts allow particle-hole excitations from the core and model space into higher orbits. These excitations are taken up to $4\hbar\omega$.

The reduced single particle matrix element becomes:

$$\langle \alpha_2 | \|\hat{T}_{JT}^\eta\| | \beta_1 \rangle = \sqrt{\frac{2T+1}{2}} \sum_{t_z} I_T(t_z) \langle \alpha_2 | \|\hat{T}_{Jt_z}^\eta\| | \alpha_1 \rangle \quad (6)$$

where:

$$I_T(t_z) = \begin{cases} 1 & \text{for } T = 0 \\ (-1)^{1/2-t_z} & \text{for } T = 1 \end{cases} \quad (7)$$

and $t_z = 1/2$ and $-1/2$ for the proton and neutron, respectively.

Elastic and inelastic electron scattering form factors in terms of angular momentum J and momentum transfer q , between the initial and final states of spin $J_{i,f}$ and isospin $T_{i,f}$, are given by:¹⁵

$$\begin{aligned} |F_J^\eta(q)|^2 &= \frac{4\pi}{Z^2(2J_i+1)} \\ &\cdot \left| \sum_{T=0,1} (-1)^{T_f-T_i} \begin{pmatrix} T_f & T & T_i \\ -T_{zf} & M_T & T_{zi} \end{pmatrix} \right. \\ &\times \langle X_f | \|T_{J,T}^\eta(q)\| | X_i \rangle \left. \right|^2 \\ &\times |F_{c.m}(q)|^2 \times |F_{f.s}(q)|^2 \end{aligned} \quad (8)$$

where T_z is the projection along the z -axis of the initial and final isospin states. $F_{fs}(q) = \exp(-0.43q^2/4)$ is the nucleon finite size (fs) form factor and $F_{cm}(q) = \exp(q^2b^2/4A)$ is the correction for the lack of translation invariance in the shell model. A and b are the mass number and the harmonic oscillator size parameter, respectively.

The single-particle energies are given by¹⁴

$$\begin{aligned} e_{nlj} &= \left(2n + l - \frac{1}{2}\right) \hbar\omega \\ &+ \begin{cases} -\frac{1}{2}(l+1) \langle f(r) \rangle_{nl} & \text{for } j = l - \frac{1}{2} \\ \frac{1}{2}l \langle f(r) \rangle_{nl} & \text{for } j = l + \frac{1}{2} \end{cases} \end{aligned} \quad (9)$$

with

$$\begin{aligned} \langle f(r) \rangle_{nl} &\approx 20A^{-2/3} \text{ MeV} \\ \hbar\omega &= 45A^{-1/3} - 25A^{-2/3} \end{aligned} \quad (10)$$

The realistic M3Y effective NN interaction, which is used in the electron scattering v_{12} , is expressed as a sum of the central potential part, v_{12}^C , spin-orbit potential part, v_{12}^{LS} , and long range tensor part, V_{12}^{TN} , as follows¹⁶

$$V_{12} = V_{12}^{(c)} + V_{12}^{(LS)} + V_{12}^{(TN)} \quad (11)$$

The two-body matrix elements of the realistic M3Y effective NN interaction consist of three parts: the central matrix element, the spin-orbit matrix element and the tensor matrix element.

$$\langle j_1 j_2 | V_{12} | j_3 j_4 \rangle_{\Gamma} = \langle j_1 j_2 | V_{12}^c | j_3 j_4 \rangle_{\Gamma} + \langle j_1 j_2 | V_{12}^{Ls} | j_3 j_4 \rangle_{\Gamma} + \langle j_1 j_2 | V_{12}^{TN} | j_3 j_4 \rangle_{\Gamma} \quad (12)$$

The reduced transition probability is related to the form factor at the photon point, which is given by¹⁷

$$B(CJ) = \frac{|(2J+1)!!|^2 Z^2 e^2}{4\pi k^{2L}} |F_J^{Co}(q=k)|^2 \quad (13)$$

where $q = k = (E_x)/(\hbar c)$ is the momentum transfer and the term $|F_J^{Co}(q=k)|^2$ is the longitudinal (Coulomb) form factor at $k = q$, which is given by

$$|F_J^{Co}(k)|^2 = \frac{4\pi}{(2J_i+1) Z^2} \left| \int_0^{\infty} dr r^2 j_J(kr) \rho_J(i, f, r) \right|^2 \quad (14)$$

Here $\rho_J(i, f, r)$ is the transition charge density for initial and final states. For the two-body matrix elements of the residual interaction $\langle \alpha \alpha_2 | V_{12} | \beta \alpha_1 \rangle_{\Gamma}$, which appear in Eqs. (5) and (11), the Michigan three Yukawas (M3Y) interaction of Bertch et al.⁴ is adopted. The interaction is taken between a nucleon in any core-orbit and a nucleon that is excited to higher orbits with the same parity and with the required multipolarity (Λ), and also between a nucleon in any sd orbits and that is excited to higher orbits with the same parity and with the required multipolarity. This interaction is given in the LS-coupling.

3. RESULTS AND DISCUSSION

A microscopic theory has been applied to calculate electron scattering form factors with CP effects using M3Y as a residual interaction for some light nuclei: ${}^6\text{Li}$, ${}^9\text{Be}$, ${}^{11}\text{B}$ and ${}^{12}\text{C}$. The OBDM elements are calculated by using the shell model NUSHELL code¹⁸ with *psdmwk* as effective interactions using large scale psd ($1p_{1/2}$, $1p_{3/2}$, $1d_{3/2}$, $1d_{5/2}$ and $2s_{1/2}$) model space. The radial wave function for the single-particle matrix elements have been calculated with the HO.

4. THE EVEN-EVEN NUCLEI: ${}^6\text{Li}$ AND ${}^{12}\text{C}$

The M1 form factors for 1^+ (0.0 MeV) state in ${}^6\text{Li}$ nucleus calculated with and without CP effects on $1p$ and large scale psd-shells wave function, see Figure 1. The solid curves and Plus-Symbol curve represent the calculation with and without CP effects, respectively, using microscopic theory with CPM3Y code. The dashed curves represent calculations with CP effects on the $1p$ model space wave function. The experimental data are taken from Ref. [19] (squares) and Ref. [20] (circles). The form factor with inclusion of the CP effect using large scale shells gives agreement in the first and second maximum diffraction,

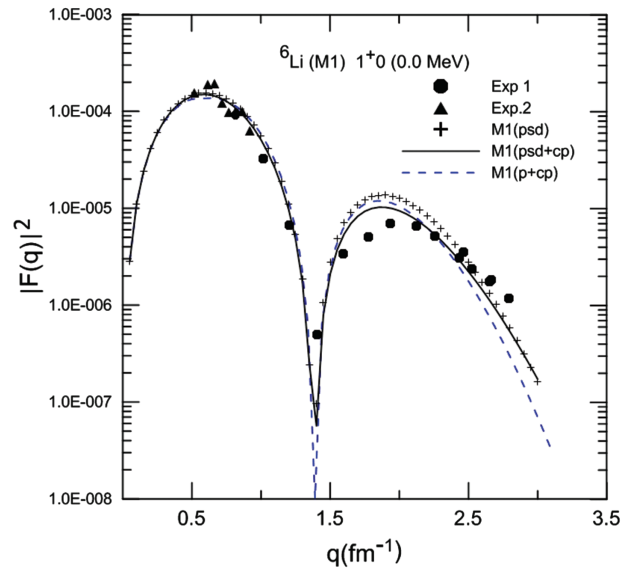


Fig. 1. Elastic M1 transverse form factors for the $1^+ 0$ (0.0 MeV) states in the ${}^6\text{Li}$ nucleus calculated with CP effects on the psd model space wave function. The experimental data are taken from Ref. [19] (squares) and Ref. [20] (circles). The solid curves and Plus-Symbol curve represent the calculation with and without CP effects, respectively, using the CPM3Y code. The dashed curves represent calculations with CP effects on the $1p$ model space wave function.

but the calculation with inclusion CP effects in $1p$ -shell doesn't affect significantly the calculation of the form factors in the momentum transfer region $q \geq 1.5 \text{ fm}^{-1}$. The transverse M1 form factors have two peaks at 0.6 and 1.82 fm^{-1} , respectively, where these peaks nearly have the same position for all calculation with and without inclusion CP effects. In general the large scale shell model calculation enhanced the calculations in the all momentum transverse region comparing with $1p$ -shell model calculations.

Figure 2 shows the transverse M1 form factors for the transition from the ground state $1^+ 0$ to $0^+ 1$ states with excitation energy 3.562 MeV for ${}^6\text{Li}$. The calculation without inclusion CP effects fails to describe the experimental data in all momentum transfer region. The form factor with CP effect using $1p$ and psd-model space give a good agreement in the first maximum diffraction. The $1p$ -shell calculation with inclusion CP effects in the second maximum diffraction fails to described between the momentum transfers region ($1.5 < q < 2.5$) fm^{-1} comparing with the experimental data.^{21,22} The large scale shell model calculations described the experimental data very well in all momentum transfer region comparing with $1p$ -shell calculations. The first and second maximum diffraction without inclusion CP effects are 0.7 and 2.1 fm^{-1} , respectively, while the first and second maximum region with inclusion CP effects are 0.5 and 1.9 fm^{-1} , respectively. From these results, we concluded that the CP effects shifted the first and second peak toward decreases momentum transfer by 0.2 fm^{-1} .

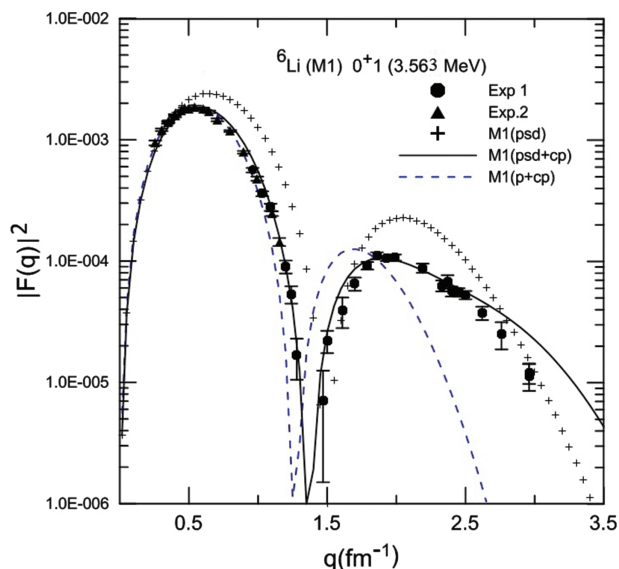


Fig. 2. Elastic M1 transverse form factors for the $0^+ 1$ state with (3.562 MeV) in the ${}^6\text{Li}$ nucleus calculated with CP effects on the psd-shell model wave function using the psd m wk effective interaction. The experimental data are taken from Ref. [21] (squares) and Ref. [22] (circles). The solid curves and Plus-Symbol curve represent the calculation with and without CP effects, respectively, using the CPM3Y code. The dashed curves represent calculations with CP effects on the $1p$ -shell model wave function.

The ${}^{12}\text{C}$ nucleus is considered as an inert ${}^4\text{He}$ core plus eight nucleons distributed over $1p_{3/2}-1p_{1/2}$ shell. The single-particle radial wave functions are those of the HO potential with size parameter $b_{\text{rms}} = 1.64$ fm. Figure 3

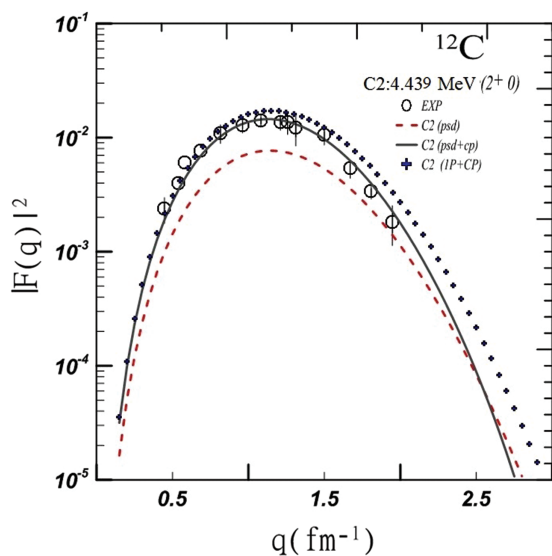


Fig. 3. Elastic longitudinal (C2) form factors for the 2^+ (4.438 MeV) state in the ${}^{12}\text{C}$ nucleus calculated with CP effects on the psd-shell model wave function using the psd m wk effective interaction. The experimental data are taken from Ref. [23]. The solid curves and dashed curves represent the calculation with and without CP effects, respectively, using the microscopic theory. The Plus-Symbol curves represent the calculation calculated with CP effects on the $1p$ -shell model wave function

shows the relation between the longitudinal form factor as a function of momentum transfer, where the dashed curve represents the results of the electron scattering form factor for $1p$ -shell model, while the solid curve represents the extended model space (psd-shells) results of the form factor with CP effect. The results of C2 form factors with extended model space and CP effect gave a clear applicability comparing with experimental data, while the results without CP effects gave a poor results. The result with $1p$ model space with CP effects as show as plus curves deviated from the experimental data²³ comparing with large scale shell mode calculations. This related that using large scale shell model with CP effects enhanced the C2 results comparing with $1p$ shell model.

5. THE ODD-A NUCLEI (${}^9\text{Be}$ AND ${}^{11}\text{B}$)

Elastic transverse (M1 + M3) form factors for the $3/2^-$ (0.0 MeV) state in the ${}^9\text{Be}$ nucleus are shown in Figure 4, where the solid curve represents the calculation of the large scale (psd) model space with CP effects by using the psd m wk effective interaction. The M3Y realistic interaction used as a residual interaction for the CP effect calculation. According to the conventional psd-shell model, it is described as an inert core of ${}^4\text{H}$ plus five nucleons distributed over psd-shell. The experimental data are taken from Refs. [19, 24]. Results are good described the momentum transfers range between (0.6–1.4) fm^{-1} , while the results with p model space causes reduced the electron scattering form factors comparing with experimental.

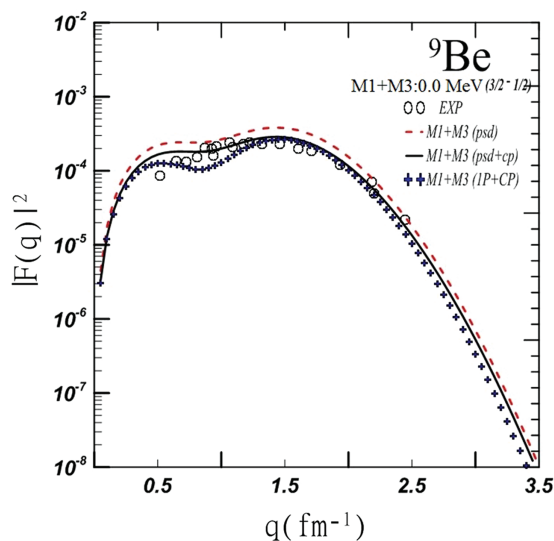


Fig. 4. Elastic Transverse (M1 + M3) form factors for the $3/2^-$ (0.0 MeV) state of the ${}^9\text{Be}$ nucleus calculated with CP effects on the psd-shell model wave function using the psd m wk effective interaction. The experimental data are taken from Refs. [19, 24]. The solid curves and dashed curves represent the calculation with and without CP effects, respectively, using the CPM3Y code. The Plus-Symbol curves represent the calculation calculated with CP effects on the $1p$ -shell model wave function.

All calculations with and without CP effects using p and psd model space give agreement with experimental data after q larger than 0.6 fm⁻¹.

Elastic longitudinal (C0 + C2) form factors for the 3/2⁻ state of the ⁹Be nucleus calculated with CP effects on the psd-shell model wave function, which are shown in Figure 5. The CP effects with the M3Y realistic interaction are included by allowing particle-hole excitation from (1p_{1/2}, 1p_{3/2}, 1d_{3/2}, 1d_{5/2}, 2s_{1/2}) shells up to higher shells with 4ħω excitations. The Psdmwk interaction has been used to calculate the multiple decompositions C0 and C2. The C0 has the dominant contribution in the entire momentum transfer region, but the contribution of the C2 (dashed curve) is added to the F_{C0}(q) (as dotted curve). The results of total transverse form factors (C0 + C2) (as a solid curves) give in a agreement, comparing with the available experimental data of Ref. [25] (circles) and Ref. [26] (triangles).

The ground state of ¹¹B is angular momentum 3/2⁻ and with isospin is 1/2. It is described in terms of seven nucleons outside a closed 1s-shell distributed over 1p_{1/2}, 2s_{1/2}, 1p_{3/2}, 1d_{5/2} and 1d_{3/2} shell. The size parameter b_{rms} = 1.611 fm is chosen from a fit to nuclear charge radius.²⁷ In this nucleus the elastic longitudinal form factors for this state is multi-polarity mixed (c₀ + c₂), which is shown in Figure 6. The CP effect with psd-shell model contributions given as a solid curve. While the C0 and C2 contributions are shown as a red dotted curves and blue dashed curves, respectively. The calculations of C0 + C2 with CP effects give good description comparing with the experimental data, especially at the momentum transfers

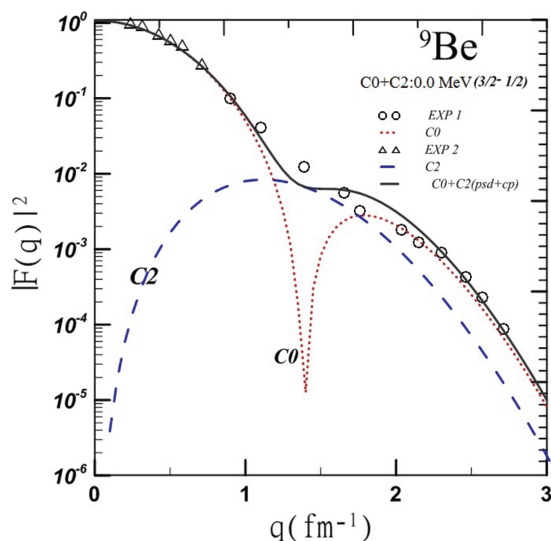


Fig. 5. Elastic longitudinal (C0 + C2) form factors for the 3/2⁻ (0.0 MeV) state in the ⁹Be nucleus calculated with CP effects on the psd-shell model space using the *psdmwk* effective interaction. The experimental data are taken from Ref. [25] (circles) and Ref. [26] (triangles). The dotted curves, dashed curves represent calculations of longitudinal C0 and C2, respectively, the solid curves represent the calculations with CP effects.

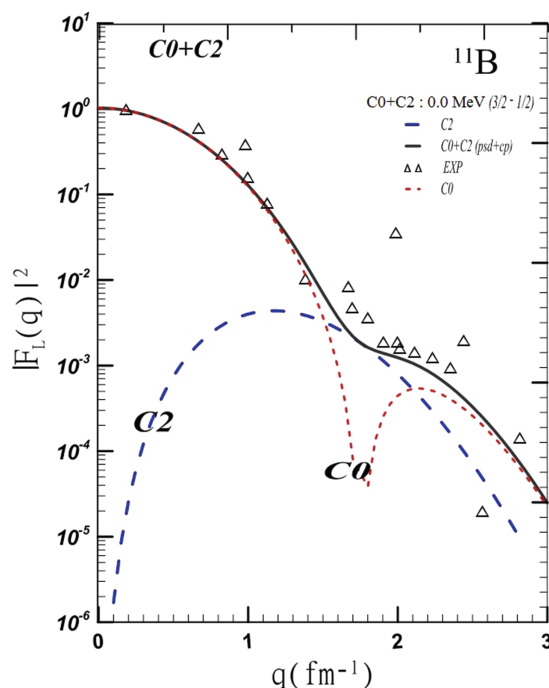


Fig. 6. Elastic longitudinal (C0 + C2) form factors for the 3/2⁻ (0.0 MeV) state in the B¹¹ nucleus calculated with CP effects on the psd-shell model wave function using the *psdmwk* effective interaction. The experimental data are taken from Ref. [27]. The dotted curves, dashed curves represent calculations of longitudinal (C0) and (C2), respectively, The solid curves and represent the calculation with C0 + C2 CP effects using the CPM3Y code.

region between (0–1.3) fm⁻¹, where the main contribution is come from C₀ multipole as show in Figure 6.

6. CONCLUSION

The elastic and inelastic electron scattering form factors for different states in the ⁶Li, ⁹Be, ¹¹B, ¹²C have been calculated taking into account higher energy configurations outside the p-shell model space with 6ħω excitation which are called CP effects. The *psdmwk* interactions for *psd*-shell are used with the M3Y effective NN interaction as a residual interaction for the CP calculations. The large scale shell model with the effect of CP give good description comparing with experimental data. The use of a modern interaction may give a better description of the form factors.

References and Notes

1. R. Roy and B. P. Nigam, Nuclear Physics. Theory and Experiment, John and Sons, New York (1967).
2. T. deForest and J. D. Walecka, *Adv. Phys.* 15, 1 (1966).
3. J. Newton, The Electromagnetic Interaction in Nuclear Spectroscopy, North-Holland (1975).
4. G. Bertsch, J. Borysowicz, H. McManus, and W. G. Love, *Nucl. Phys. A* 284, 399 (1977).
5. K. S. Jassim, A. A. Al-Sammarrae, F. I. Sharrad, and H. Abu Kassim, *Phys. Rev. C* 89, 014304 (2014).
6. K. S. Jassim and Z. M. Abdul-Hamza, *Armenian Journal of Physics* 7, 4 (2014).

7. K. S. Jassim, *Chin. J. Phys.* 51, 3 (2013).
8. K. S. Jassim, *Phys. Scr.* 86, 035202 (2012).
9. K. S. Jassim and Hasan abu Kassim, *Rom. Jour. Phys.* 58, 320 (2013).
10. K. S. Jassim, R. A. Radhi, and N. M. Hussain, *Pramana-J. Phys.* 86, 87 (2016).
11. F. A. Majeed and L. A. Najim, *Indian Journal of Physics* 89, 611 (2015).
12. Z. Wang, Z. Ren, T. Dong, and C. Xu, *Phys. Rev. C* 90, 024307 (2014).
13. R. A. Radhi and A. Bouchebak, *Nucl. Phys. A* 716, 87 (2003).
14. P. Brussaard and P. W. M. Glademans, *Shell-Model Application in Nuclear Spectroscopy?*, North-Holland Publishing Company, Amsterdam (1977).
15. T. W. Donnelly and I. Sick, *Rev. Mod. Phys.* 56, 461 (1984).
16. H. Nakada, *Phys. Rev. C* 68, 86 (2003).
17. B. A. Brown, B. H. Wildenthal, C. F. Williamson, F. N. Rad, S. Kowalski, H. Crannell, and J. T. O'Brien, *Phys. Rev. C* 32, 1127 (1985).
18. B. A. Brown and W. D. Rae, MSU-NSCL Report (2007).
19. L. Lapikas, G. Box, and H. DeVries, *Nucl. Phys. A* 253, 324 (1975).
20. J.C. Bergstrom and S. B. Kowalski, *Phys. Rev. C* 25, 1156 (1982).
21. J. C. Bergstrom, I. P. Aure, and R. S. Hicks, *Nucl. Phys. A* 251, 401 (1975).
22. J. C. Bergstrom, U. Deutschmann, and R. Neuhausen, *Nucl. Phys. A* 327, 458 (1979).
23. J. B. Flanz, R. S. Hicks, R. A. Lindgrens, G. A. Peterson, A. Hotta, B. Parker, and R. C. York, *Phys. Rev. Lett.* 41, 1642 (1978).
24. R. E. Rand, R. F. Frosch, and M. R. Yearian, *Phys. Rev.* 144, 859 (1966).
25. J. P. Glickman, W. Bertozzi, T. N. Buti, S. Dixit, F. W. Hersman, C. E. HydeWright, M. V. Hyns, R. W. Lourie, B. E. Norum, J. J. Kelly, B. L. Berman, and D. J. Millener, *J. Phys. Rev. C* 43, 2740 (1991).
26. J. A. Jansen, R. Th. Peerdeman, and C. Devries, *Nucl. Phys. A* 188, 337 (1972).
27. T. W. Donnelly and I. Sick, *Rev. Mod. Phys.* 56, 461 (1984).

Delivered by Ingenta to: Myson Hawthorne
IP: 141.217.172.167 On: Fri, 14 Oct 2016 20:03:10
Copyright: American Scientific Publishers